A Preliminary Study of Appling a Dual-Reflectivity Thresholds Technique on Storm Identification and Tracking from QPESUMS Mosaic Data

Yu-Chieh Yeh Wei-Yu Chang Hsiu-Wei Hsu
Department of Atmospheric Sciences, National Central University

Abstract

Mesoscale convective system (MCS) plays an important role in contributing heavy precipitation events in Taiwan. To investigate various structural evolutions characteristics, dynamic, microphysical processes of these precipitation systems efficiently, a storm identification and tracking technique using radar data is required. A storm with continuous region exceeding thresholds for both reflectivity and size is identified from CWB QPESUMS mosaic radar data. Two reflectivity thresholds were applied to distinguish a storm region. Lower reflectivity threshold captures entire precipitation system, the higher reflectivity threshold on the other hand captures the core of the convective system. The dual-reflectivity threshold technique distinguishes 'child-cell' (convective core zone) from 'mom.-cell' (complete precipitation area). After identifying child-cell and mom.-cell, the storm properties including geometric centroid (X, Y), reflectivity-weighted centroid (X_z, Y_z), size (A), major and minor axes ($r_1 and\ r_2$), and the orientation of the major axes relative to the x axis (θ) are analyzed. These properties thus are further examined with the evolution of the storm track. Preliminary results of a Mei-Yu front event show that the dual-reflectivity threshold technique can better capture characteristics of multicell. The number of child-cell that included in one mom.-cell is within the range of 1 to 950. In terms of the storm properties, by changing the axis ratio thresholds for mom.-cell only, most of the orientation of mom.-cells and child-cells falls in the range between -30 to 50 degree and -40 to 50 degree respectively. As regards to tracking result, using reflectivity-weighted centroid to do cell track perform better than using geometric centroid.

Keywords: Mei-Yu front, Storm Identification, Storm Tracking

1. Introduction

Over the past few decades, many of the techniques have been developed to identify convective and stratiform region by applying thresholds for both reflectivity and size. By classifying the precipitation into different rainfall types, we can know more about cloud physics or even microphysics process.

Dixon and Wiener (1993) present a methodology of thunderstorm real-time identification and tracking based on volume-scan radar data by giving a threshold for both storm size and speed. Steiner et al. (1995) tested some algorithms to separate the radar echo into different precipitation area, using three revised criteria for identifying convective precipitation grid point. In their study, the influence radius and the threshold are functions of area-averaged background reflectivity. Yang et al. (2013) developed a fuzzy logic (FL) algorithm to classify convective and stratiform rainfall based on radar reflectivity observations. By setting the membership function, the FL algorithm can express the classifications in a probabilistic way.

The algorithm presented here is based on Dixon and Wiener (1993) storm identify and tracking. Different to their method, two reflectivity thresholds were set. Lower threshold to distinguish the possibility of precipitation area, while higher threshold to guarantee the storm that belongs to convective system instead of a widespread stratiform. The foci of this study are to apply the dual-reflectivity threshold technique on different time resolution radar data, to confirm the truth of better tracking result on higher time continuity.

2. Data Preparation

Two kinds of data were used in this study. QPESUMS mosaic radar data from Central Weather Bureau on 21 May 2014 were in Cartesian coordinates at 0.0125-degree resolution and 10 minutes time resolution. Composite reflectivity data from Kaohsiung LinYuan weather radar (RCLY) on 21 May 2020 were transformed from radar coordinate into Cartesian coordinates, with 1-kilometer horizontal resolution and 0.5-kilometer vertical resolution in 150-kilometer radar radius.

For data quality controls of RCLY, factors taken into consideration include the following: (a) remove near radar data (b) standard deviation thresholds (c) unfold PhiDP (d) attenuation correction (e) system bias correction. This process has been well tested, undoubtedly, it performs the best result.

3. Methodology

A. Storm identification

In this study, two reflectivity thresholds (T_z) were applied to distinguish a storm region. To investigate the sensitivity of the precipitation area to the reflectivity threshold. T_z was test from 15 to 35 dBZ with 5 dBZ interval. Obviously, the 15-dBZ can capture the entire system scope, included both convective and stratiform precipitation types. On the contrary, the 35-dBZ can capture smaller reflectivity field but the core of the convective system.

To deal with the complexity of the Mesoscale convective system, selecting only one threshold for reflectivity appears not to be an ideal process for storm identification. Consequently, the idea of dual-reflectivity thresholds technique was born. It is designed to capture the complete precipitation system only when the convective core existed.

Based on the results of the initial experiments, Lower reflectivity threshold ($T_{z,mom}$) and higher reflectivity threshold ($T_{z,child}$) was set to 20 and 35 dBZ for the thresholds of QPESUMS Mei Yu case study, 30 and 35 dBZ for the final thresholds of RCLY case study. Three different storm identification result were produced. $T_{z,mom}$ for 'mom cell', $T_{z,child}$ for 'child cell' and the cell content both convective system core and precipitation area for 'cell left'.

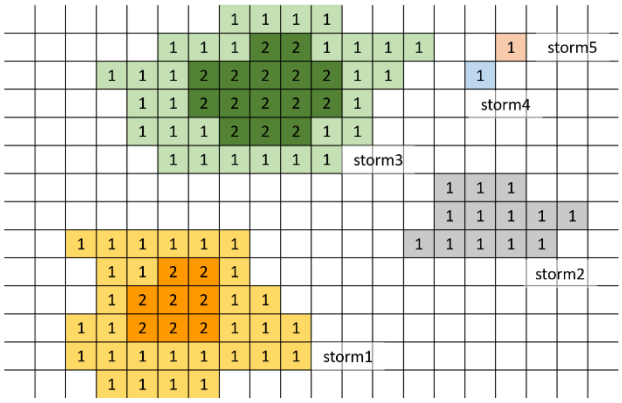

FIG.1. Example of storm identification. Different color in different shape indicates different storms which grid points exceed given reflectivity thresholds. Lighter shading with number '1' for the reflectivity exceed $T_{z,mom}$. Darker shading with number '2' for the reflectivity exceed $T_{z,child}$.

Figure 1 depicts the storm identify results. Storm 1 and Storm 3 represent child-cell within mom-cell, here after 'cell left'. Storm 2, 4, 5 indicate mom-cell without child-cell. Obviously, once a child-cell exist, mom-cell exist. Furthermore, a mom-cell may carry more than one child-cell when the storm is defined as 'multicell'.

For the purposes of storm tracking and analysis, storm properties were computed, including geometric centroid (X, Y), reflectivity-weighted centroid (X_z, Y_z), size (A), major and minor axes ($r_1 and\ r_2$), and the orientation of the major axes relative to the x axis (θ) are analyzed.

B. Storm tracking

Applying storm properties in different time interval (Δt) between time 1 (t_1) and time 2 (t_2) will cause varied in tracking results. On this account, we attempted to modify Δt from 10 minutes to 2 minutes. In order to prove that the higher time resolution, the more accurate storm track will be.

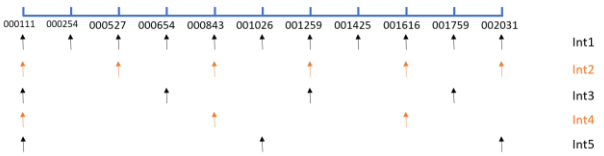

FIG.2 An example of data time resolution strategy.

Before storm tracking, we will first encounter the issue of unequal interval radar scan volume time. The biggest difference from CWB mosaic radar data is that the RCLY data time interval are approximately 2 minutes, but for CWB mosaic radar data, the time interval are absolutely 10 minutes. Therefore, to deal with this problem, we decided to input the data with given data number interval rather than given specified time interval. As Figure 2, top eleven data time are shown, each arrow represents the data we input for storm tracking. For example, Int1, we input all of the radar data from 000111 UTC to 015229 UTC (Δt ≅ 2 mins). It's worth noting that the time intervals of Int5 are about 10 minutes, correspond to the time interval of CWB mosaic radar data. With different time interval, we can clearly see the impact on tracking result.

Based on Dixon and Wiener (1993) present, three assumptions were set to track the storms at t_1 and t_2.

(1) The similarity of storm properties.
(2) The shorter path, the more likely to be a true one.
(3) Governed by maximum expected speed (S_{max}).

In our initial experiments, we had also tested storm track with both (X, Y) and (X_z, Y_z). It shows a more reasonable result by applying the reflectivity-weighted centroid rather than geometric centroid. Therefore, we will adopt reflectivity-weighted centroid (X_z, Y_z) for storm tracking and set S_{max} to 30 $^{m}/_{s}$ in this paper.

4. Results and Discussions

In order to verify our dual-reflectivity threshold technique performed well, two Mei-Yu case were chosen. The purpose to chose Mei-Yu front is because it is classified as a multicell. If we select a case of single cell, we can't distinguish the difference between mom-cell and child-cell, the result of storm identification and tracking will be parallel.

A. Case 1: 21 May 2014

Figure 3 shows an example of storm identification with different reflectivity threshold. The radar mosaic over Taiwan shows a large area of $Z_h > 20$ dBZ. While only 8 mom-cell is defined in fig.3c, but 84 child-cell in fig.3b. Obviously, one mom-cell can include 60 child-cell at this time. Figure 4 shows the calculation of how many

child cells that belongs to the same mom-cell. For example, the green circle on the left top of the Figure, illustrate there is one mom-cell that include 64 child-cell in the whole day. The slope (red line) in the Figure shows the relationship between child-cell number within mom-cell number of this case. Due to multicell, negative slope appears. Ones if the system is classified as single cells, the slope will become "1". That is, there is only one child-cell within each mom-cell. Thunder storm is a prime example of it.

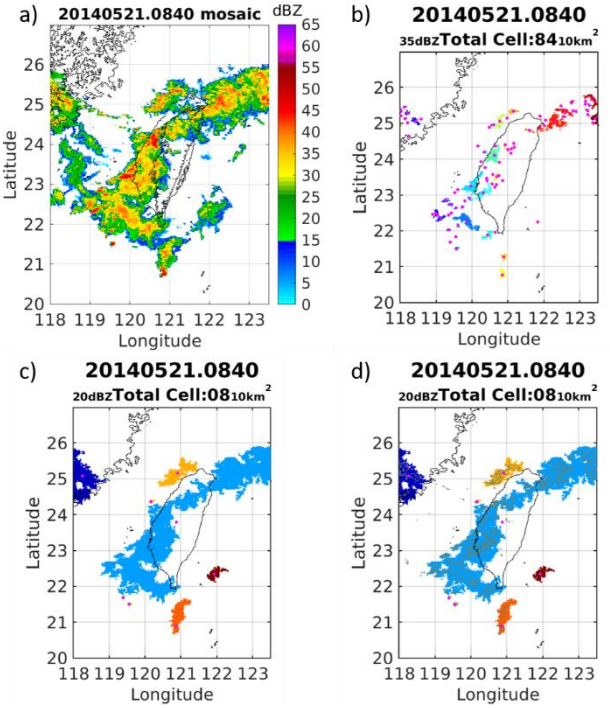

FIG. 3. Case study 1 of Mei Yu case at 0840 UTC 21 May 2014 with (a) QPESUMS mosaic data (b) child-cell storm identification (c) mom-cell storm identification and (d) cell-left storm identification, contour lines for 35-dBZ area. Different color represents different area of storms, pink dot for reflectivity-weighted centroid (X_z, Y_z) of each storm.

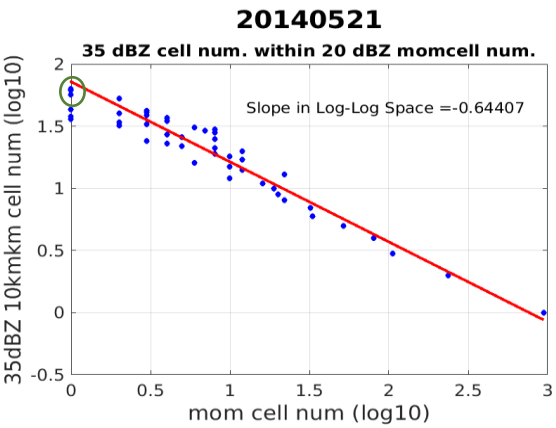

FIG.4. Counts for number of child-cell within one mom-cell in log 10 scale. Red line shows the slope of this case.

For more analysis of storm properties, Figure 5 shows the relationship between each storm's axis ratio and orientation. It is obvious that the maximum of axis ratio from fig5(a) has a border range compare with fig5(b), most of the axis ratio lies between 0.3 to 0.6 for mom-cell and 0.4 to 0.6 for child-cell.

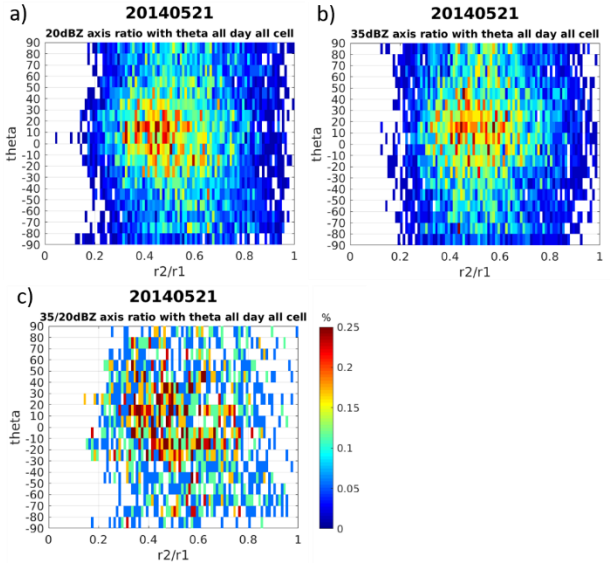

FIG.5. An initial analysis of axis ratio and orientation in one day for (a) mom-cell (b) child-cell (c) cell-left. X-axis is the axis ratio and y-axis for the orientation.

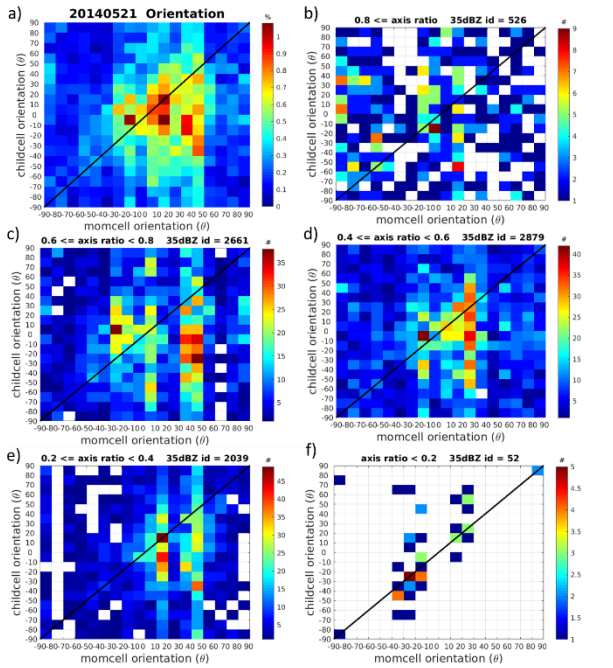

FIG.6. Calculate the orientation between mom-cell and child-cell for all day by changing the axis ratio threshold (T_{axis}) for mom-cell only. (a) All data (b) $T_{axis} \geq 0.8$ (c) $0.6 \leq T_{axis} < 0.8$ (d) $0.4 \leq T_{axis} < 0.6$ (e) $0.2 \leq T_{axis} < 0.4$ (f) $T_{axis} < 0.2$.

For more detail analyses, Figure 6 shows the result from changing threshold for mom-cell axis ratio. For instance, Figure 6(b), only calculate the axis ratio exceed 0.8 for mom-cell, but entire data set from child-cell. From Figure 6(a), we know that most of the mom-cells present the trend of northeast to southwest, consistence with our cognition to the Mei-Yu Front in Taiwan. In Figure 6(c)~6(e), most of the orientation of mom-cell lies between 30 to 50 degree, with not much distinct features

in child-cell. We consider it is because the area of child-cell is not big enough, once a tiny change on the boundary, the orientation will have a significant change.

B. Case 2: 21 May 2020 (000111 ~ 015229 UTC)

With the result of Case 1, we discover setting the threshold to 20-dBZ for mom-cell captured too wide storm area, leading the result to have too many child-cells in a huge mom-cell. To solve this problem, we change the reflectivity threshold to 30-dBZ for mom-cell. The purpose of this section is to explore how the data time resolution influence storm tracking result.

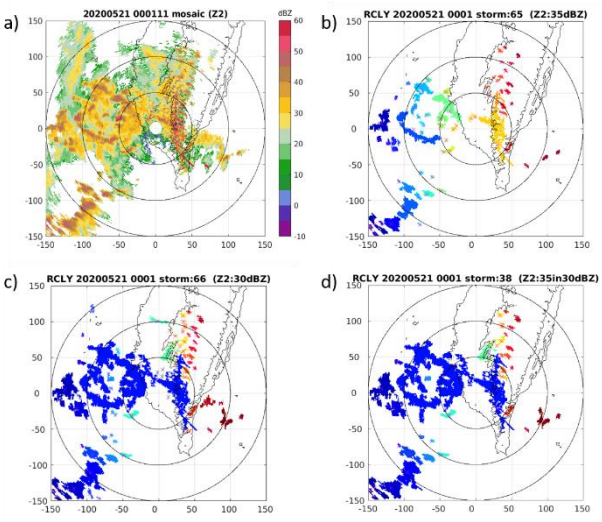

FIG.7. Case study 2 of Mei Yu case at 000111 UTC 21 May 2020 of RCLY with (a) mosaic data (b) child-cell storm identification (c) mom-cell storm identification and (d) cell-left storm identification. Different color represents different area of storms, pink dot for reflectivity-weighted centroid (X_z, Y_z) of each storm. Unit of distance: kilometer.

The starting time RCLY radar mosaic data and storm identification results, including mom-cell, child-cell and cell-left, are shown in Figure 7. We can find that, although we did the quality control on radar data, there are still some ground clutter at Central Mountains Range. By the characteristic of ground clutter, strong reflectivity and motionless, we can treat it as a reference, to examine the correctness of tracking results.

Figure 8 shows the tracking result for mom-cell in different time integer. From Figure 8(a) to 8(e), as the time resolution becomes longer, the results turns terrible, especially over the Central Mountains Range. Same phenomenon also appears at child-cell and mom-cell (not shown here).

For more detailed discussions, Figure 9 shows an example of the longest track of the entire analysis time. Different line color represents different data time integer, from Int1 to Int5. Here, we set Int1 for our reference due to the highest time resolution. Visibly, Int2 and Int3 are more consistent with Int1. Int4 track a wrong storm at the third time point. Although Int5 track path is coincide with Int1, the storm lifetime is much shorter and end at the third time point.

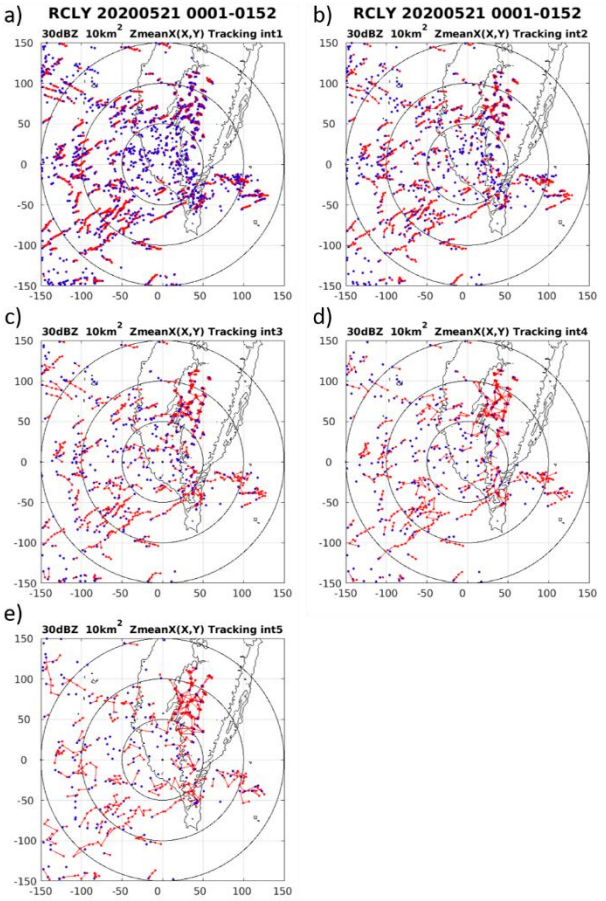

FIG.8. Storms track result from 000111 UTC to 015229 UTC for mom-cell only. (a)~(d) for different input data time resolution. (a) Int1 ($\Delta t \approx 2$ mins), (b) Int2 ($\Delta t \approx 4$ mins), (c) Int3 ($\Delta t \approx 6$ mins), (d) Int4 ($\Delta t \approx 8$ mins), (e) Int5 ($\Delta t \approx 10$ mins). Blue dot: starting point of each storm track. Red line: different track path.

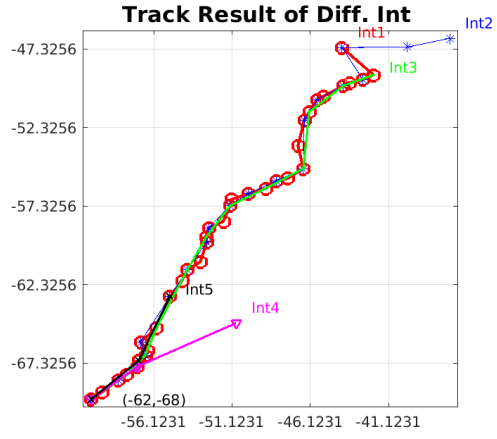

FIG.9. An example of comparing the difference in tracking result between Int1~Int5 for mom-cell. Red line: Int1. Blue line: Int2. Green line: Int3. Pink line: Int4. Black line: Int5. $(-62, -68)$ is the starting point. Coordinate points represent the position relative to the RCLY radar.

5. Conclusion and Future Prospects

We present a new storm identification technique in

this paper. Three identify result will be produce in one time, mom-cell, child-cell and cell-left. By inputting different time resolution or reflectivity data, dissimilar tracking result will be produced.

In this study, we choose two different form of radar data to reveal the result of our technique. Case 1, a Mei-Yu case of CWB mosaic radar data, 20-dBZ and 35-dBZ reflectivity thresholds were applied. The result present in Figure 3~6, proved the dual-reflectivity technique works well. We can not only distinguish the core of convective system (child-cell) by higher reflectivity threshold but also the entire precipitation area (mom-cell) by lower reflectivity threshold. Storm properties of each cells are also been calculated. By counting their characteristics, we can learn more about the system at that time.

However, we than found that the threshold of mom-cell is inappropriate. It captures too many precipitation areas that we are not interested. Therefore, we changed the reflectivity threshold of mom-cell from 20-dBZ to 30-dBZ and stay the same threshold (35-dBZ) for child-cell. Figure 7~9 shows the result of changed reflectivity of case 2, a Mei-Yu case of RCLY data form. In this case, we change the data input time resolution from Int1 (≈ 2 mins) to Int5 (≈ 10 mins) to storm track. The tracking results are consistent with us acknowledge, better outcome for higher time resolution, unsatisfactory results for lower time resolution.

From an example in Figure 9, we can see that not all the tracking result performed worst. Int2 and Int3 shows similar track path to Int1, however Int4 and Int5 don't. In our future prospects, we are looking forward to improve our tracking formula, hope to see the improvement on Int4 and Int5.

6. References

陳新淦, 黃椿喜, 呂國臣, 洪景山, and 張博雄, 2016: 利用雷達回波影像辨識及篩選技術發展極短期系集定量降水預報, **44,** 1-31.

Dixon, M. and Wiener, G. 1993: TITAN: Thunderstorm Identification, Tracking, Analysis, and Nowcasting – A Radar-based Methodology, *J. Atmos. Oceanic Technol.*,**10,** 785-797.

Fridlind, A. M., and Coauthors, 2019: Use of polarimetric radar measurements to constrain simulated convective cell evolution: a pilot study with Lagrangian tracking. *Atmos. Meas. Tech.*, **12,** 2979-3000.

Parker, M., and Johnson, R. H. 2000: Organizational Modes of Midlatitude Mesoscale Convective Systems, **128,** 3413-3436.

Steiner, M., R. A. Houze, Jr., and S. E. Yuter, 1995: Climatological Characterization of Three-Dimensional Storm Structure from Operational Radar and Rain Gauge Data. *Journal of Applied Meteorology*, **34,** 1978-2007.

Yang, Y., Chen, X., and Qi, Y. (2013), Classification of convective/stratiform echoes in radar reflectivity observations using a fuzzy logic algorithm, *J. Geophys. Res. Atmos.*, **118,** 1896– 1905.